Post-Translational Modification of Bionanoparticles as a Modular Platform for Biosensor Assembly

Qing Sun, Qi Chen, Daniel Blackstock, and Wilfred Chen*

Department of Chemical and Biomolecular Engineering, University of Delaware, Newark, Delaware 19716, United States

ABSTRACT Context driven biosensor assembly with modular targeting and detection moieties is gaining significant attentions. Although protein-based nanoparticles have emerged as an excellent platform for biosensor assembly, current strategies of decorating bionanoparticles with targeting and detection moieties often suffer from unfavorable spacing and orientation as well as bionanoparticle aggregation. Herein, we report a highly modular post-translational modification approach for biosensor assembly based on sortase A-mediated ligation. This approach enables the simultaneous modifications of the *Bacillus stearothermophilus* E2 nanoparticles with different functional moieties for antibody, enzyme, DNA aptamer, and dye decoration. The resulting easy-purification platform offers a high degree of targeting and detection modularity with signal amplification. This flexibility is demonstrated for the detection of both immobilized antigens and cancer cells.

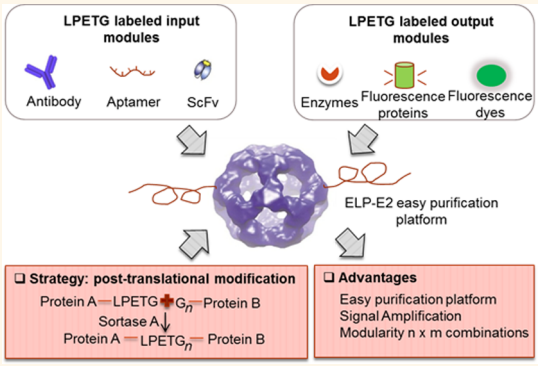

KEYWORDS: biosensor · post-translational modification · bionanoparticles · modularity · signal amplification · easy purification

Analytes, including pathogens,[1,2] toxins,[3−5] tumor markers,[6,7] and metabolites,[8] have attracted substantial attentions due to their impact on human health and daily lives. Biosensors, which employ biological elements to convert the recognition of analytes into detectable signals, have been widely used for monitoring biorecognition events.[9] The most common biosensor format employs a target-specific primary antibody for recognition and the use of secondary antibodies modified with either fluorescence dyes or enzymes to reflect the initial binding events.[10] Direct labeling of primary antibodies has also been reported, however, this method suffers from tedious chemical modifications, reduced binding affinity, and limited sensitivity.[11] Ideally, a universal adaptor platform that is able to link any recognition motif of interest to a detection module is of great interest, especially if signal amplification can be achieved to detect analytes with the required sensitivity.[6]

Recently, a bifunctional adaptor with the ability to link immunoglobulin G (IgG) to different DNA-modified output domains was constructed to achieve a high degree of modularity and selectivity.[10] Significantly improved target interaction and detection sensitivity have also been achieved by using complex three-dimensional nanoscaffolds, allowing dual modifications with IgGs and quantum dots (QDs).[6] This improved sensitivity is the result of signal amplification achieved by linking multiple QDs to a single binding event. A similar enhancement in detection sensitivity has been reported by immobilizing multiple biotin-conjugated antibodies and invertases onto streptavidin magnetic beads. Binding of a single bead onto targets resulted in the conversion of sucrose to glucose by multiple invertases for highly sensitive detection.[12]

Among different nanoscaffolds, protein-based nanoparticles are the most attractive as they offer the ability to self-assemble from simple uniform-size protein building blocks and allow precise control over material architectures.[9] Despite these desirable properties, protein bionanoparticles do have several drawbacks. Most noticeably is the use of chemical modifications for functionalization, which can result in random

* Address correspondence to wilfred@udel.edu.

Received for review June 17, 2015 and accepted August 2, 2015.

Published online August 03, 2015
10.1021/acsnano.5b03688

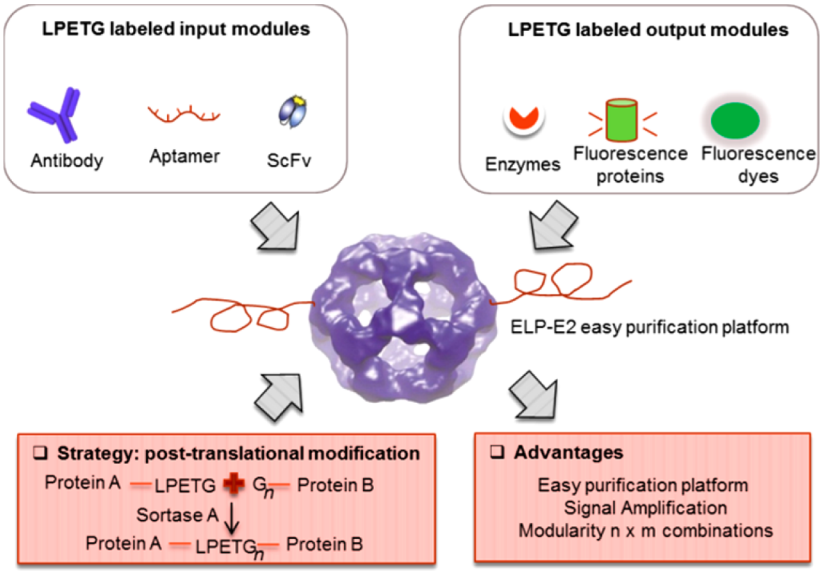

Figure 1. Schematic of sortase A (SrtA)-mediated modification of ELP-E2 nanoparticles for sensor assembly. A LPETG tag is added to the C-terminus of the different sensing and detection modules for ligation with the N-terminal tri-glycine tag of E2. Signal amplification and modularity are the expected outcome advantages of this system.

orientation and loss of functions.[13−17] Direct genetic fusion has been previously reported by fusing protein G and a His6-tag onto the surface of apoferritin to capture antibodies and nickel-nitriolotriacetic acid (Ni-NTA) coated quantum dots, gold particles or magnetic particles for sensor assembly.[6] However, genetic fusion is limited to relative small peptides and proteins, restricting the varieties of sensing and detection moieties that can be decorated.[18,19] As a result, the ability for simultaneous modifications with multiple sensing and detection modules remains challenging. Ideally, a universal approach to interface different sensor components in the correct spatial orientation will be invaluable to satisfy the need to create highly modular biosensing platforms.[10]

Staphylococcus aureus Sortase A (SrtA) is a bacterial transpeptidase that catalyzes the condensation reaction between a C-terminal LPXTG recognition motif and an N-terminal tri-glycine tag to generate a native amide bond.[20,21] The N to C ligation can be used to guarantee the spatial orientation of targeted moieties, while the small size of the tags has a minimal impact on functionalities. Since the ligation can proceed at mild pH and temperature conditions,[22] we argue that SrtA can be exploited to attach multiple proteins and peptides onto protein nanoparticles without any effect on folding and functionalities.

Our group has recently demonstrated this feasibility of attaching multiple proteins onto the E2 core of the pyruvate dehydrogenase complex from *Bacillus stearothermophilus*,[23] a genetically modifiable 60-mer protein bionanoparticle of 24 nm diameter.[24,25] Simple recovery of modified E2 nanoparticles was achieved using two cycles of thermal precipitation and resolublilization by taking advantage of the tethered thermal-responsive elastin-like-polypeptide (ELP) moiety.[23,26,27] This thermal based purification scheme enables recovery of bionanoparticles within 1 h without the use of conventional sucrose gradient, ultracentrifugation or chromatography that are time-consuming and expensive.[28,29] Because of the versatility in decorating E2 with proteins of different sizes and properties and the ease in purification, this approach is ideal in transforming E2 into a modular sensing platform capable of facile exchange and integration of different targeting and detection components. To illustrate this modularity, we modified the E2 nanoparticles with a combination of the antibody-binding Z domain,[30] the DNA- or fluorescent dye-conjugating HaloTag,[31,32] and nanoluciferase (Nluc)[33] to form highly specific and sensitive biosensors for the detection of antigens and cancer cells (Figure 1, Figures S1 and S2).

RESULTS AND DISCUSSION

The E2 core is composed of 60 identical monomers that self-assemble into a highly stable cage-like structure (Figure S3A).[24,25] A tri-glycine tag was added to the N-terminus of the E2 monomer and up to 60 different protein moieties can potentially be ligated onto a single E2 nanoparticle. Antibody, one of the most commonly used binding motif, was chosen as the initial recognizing module. Since it is difficult to modify each target antibody individually, an antibody capturing Z domain, a shorter synthetic domain derived from the *S. aureus* protein A, was used for antibody immobilization. The Z domain has a reported binding affinity of 10 nM to the Fc region and can be used to properly orient IgG without affecting accessibility of the Fab domain.[30] To achieve high level expression, the Z domain was fused to a thermally stable carrier protein,

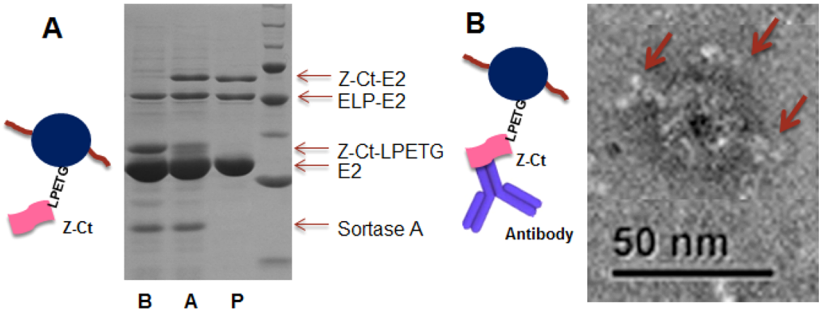

Figure 2. Sortase A-mediated Z-Ct-LPETG ligation onto ELP-E2 cage. (A) SDS-PAGE analysis of reaction mixtures before (B) and after (A) ligation as well as purified products (P). (B) Transmission electron micrograph of IgG-bound E2 nanoparticles. Y-shaped IgGs were shown to bind onto intact E2 nanoparticles.

cohesin Ct from *Clostridium thermocellum*.[34] A LPETG tag was added to the C-terminus of Ct for SrtA ligation. Expression of Z-Ct-LPETG fusion was confirmed by SDS-PAGE analysis (Figure S4A). One added benefit of using a thermally stable partner is the ability to purify the fusion protein by incubating at 70 °C for 10 min to denature most other cellular proteins (Figure S4A). The flexibility to choose any fusion partner of interest without size limitation is another advantage of post-translational modification compared with direct fusion.

ELP-E2 conjugates were first prepared by StrA ligation as reported previously (Figure S2A).[23] Next, Z-Ct-LPETG was further ligated onto purified ELP-E2 to form Z-ELP-E2 conjugates and purified again using two cycles of thermal precipitation and resolubilization. The final purified product was verified by SDS-PAGE analysis and a new band corresponding to Z-Ct-E2 was detected (Figure 2A). From the band density analysis, about 5 Z-Ct-LPETG were ligated per E2 cage for antibody capture. To check the function of ligated Z-domains, rabbit IgGs were incubated with Z-ELP-E2 nanoparticles at a 3:1 ratio and thermal purification was used to remove unbound antibodies. Successful capturing of IgGs was confirmed by detecting bands corresponding to the heavy chain fragments (Figure S4B) after binding and purification. Transmission electron micrograph (TEM) images further confirmed the capture of Y-shaped IgGs by the ligated Z domain (Figure 2B and S3B).

In many sensitive immunoassays, enzyme is a popular choice as the sensor output due to the ability to amplify signals through enzyme activity. NanoLuc (Nluc) luciferase is a small (19.1 kDa) monomeric luminescent reporter enzyme engineered from deep sea *Oplophorus gracilirostris*.[33] Nluc is an ATP-independent luciferase, about 150-fold brighter than either firefly (*Photinus pyralis*) or *Renilla reniformis* luciferase. Since it is a thermally stable enzyme with a melting temperature of 58 °C, we were able to partially purify Nluc-LPETG by incubating cell lysis at 55 °C (Figure S5A). Nluc was ligated onto ELP-E2 nanoparticles and purified as described above (Figure S5A). The Nluc conjugates were fully functional as verified by the detection of luminescence (Figure S5B).

With the individual sensing and detection components expressed and ligated onto the ELP-E2 nanoparticle, the first generation of biosensor was assembled using the Z-domain for antibody capturing and Nluc as the detection module. To generate this multifunctional particle, a sequential ligation procedure was employed to control the decoration efficiency of the individual component in each step. Z-Ct-LPETG was first ligated onto ELP-E2 to form Z-ELP-E2, followed by the ligation of Nluc-LPETG to assemble the Z-ELP-E2-Nluc conjugates (Figure 3A). This sequential ligation strategy was utilized to provide a decoration efficiency of 5 Z domains and 5 Nluc per nanoparticle, which could provide up to 5 times signal amplification upon antibody binding (Figure S6A). Dynamic light scattering confirmed the correct nanoprobe assembly as the particle size increased from 32 nm for Z-ELP-E2 to 40 nm for the IgG-Z-ELP-E2-Nluc conjugate (Figure S6B).

To test the functionality of assembled biosensors, thrombin, a human protease involved in the coagulation cascade for anticlotting therapeutics, theombosis and heamostatis, was used as the analyte.[35,36] As a control, a fusion protein with the Z domain in the N-terminus, Nluc in the C- terminus, and ELP in between as a linker for purification, was constructed (Figure 3A and Figure S6C). As expected, both constructs were successful in detecting 10 nM thrombin. However, the signal was 5-fold higher with the E2 nanoprobe, a result consistent with the 5 times higher ratio of Nluc per nanoparticle (Figure 3B).

To further investigate whether we can adjust the level of signal amplification, we took advantage of the two-step ligation procedure to fix the amount of Z-Ct ligated on ELP-E2 while varying the decoration efficiency of Nluc in the second step by changing the reactant concentration (Figure 3C). Densitometry analysis revealed that up to 22 Nluc per nanocage was achieved (Table S2). With the use of this series of E2 nanoprobes for thrombin detection, a corresponding increase in the signal amplification was detected with increasing ratios of Nluc per nanoprobe (Figure 3D). This result highlights the flexibility in fine-tuning the signal amplification by changing the detection module

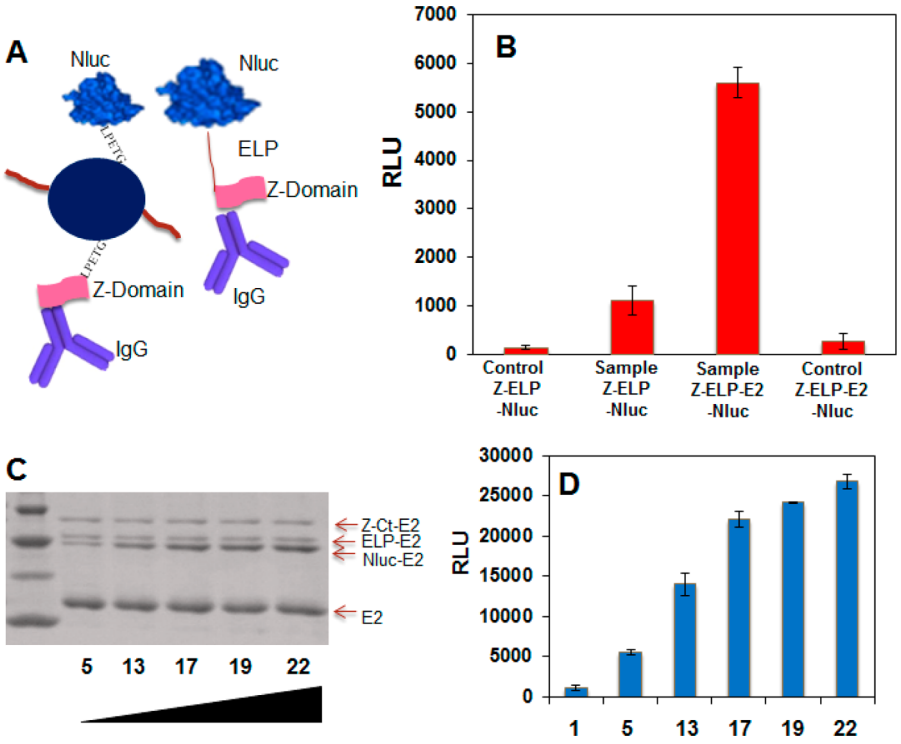

Figure 3. E2 nanoprobes assembly with antibodies captured by the Z domain for sensing and Nluc for detection. (A) Schematic representations of IgG-Z-ELP-E2-Nluc and IgG-Z-ELP-Nluc. (B) Thrombin detection with Z-ELP-Nluc fusion proteins and IgG-Z-ELP-E2-Nluc nanoprobes; control samples contained no thrombin. (C) Signal amplification using controlled Nluc assembly by conjugating varying numbers of Nluc (5−22) onto E2 nanoparticles. (D) Detection of thrombin using E2 nanoprobes with varying Nluc decoration efficiencies.

decoration efficiency. Using the nanoprobes containing 22 Nluc, we further investigate the sensitivity of the assay. As low as 2.5 nM thrombin was easily detected (Figure S6D); this detection limit is in line with other reported enzyme-based ELISA assay for thrombin.[37−39]

We next demonstrated the utility of E2 nanoprobes for the detection of cancer cells. MUC1, a cell surface associated glycoprotein, was chosen as the target, whose overexpression was associated with a variety of breast, ovarian, lung, and pancreatic cancers.[40,41] A well-characterized anti-MUC1 antibody was loaded onto our nanoprobes to detect the surface-exposed MUC1 markers on fixed HeLa cells (Figure 4A). A significant Nluc activity was detected only with antibody-loaded nanoprobes, while no signal was observed for the control nanoprobes without antibodies (Figure 4B).

While very sensitive, this Nluc-based assay cannot be easily adapted to traditional microscopy imaging for cancer detection.[42] To address this problem, we replaced Nluc with Alexa 488 as the output while keeping the Z-domain for antibody capture. HaloTag, a modified haloalkane dehalogenase capable of linking a suicide chlorohexane (CH) ligand covalently to the protein, was employed to conjugate CH-modified Alexa 488.[31] The expression of HaloTag-LPETG was confirmed by SDS-PAGE (Figure S7A), and the successful ligation of HaloTag onto ELP-E2 was achieved (Figure S7A). The functionality of the ligated HaloTag was further demonstrated by the ability to conjugate with CH-modified Alexa 488 (Figure S7B). By simply replacing Nluc with HaloTag in the second step of the sequential ligation reaction, a new nanoprobe composed of the MUC1 antibody and Alexa 488 was constructed to visualize fixed HeLa cells (Figure S7C). Again, brightly fluorescent cells were detected only with nanoprobes loaded with antibodies (Figure 4C). This example highlights the modularity of our approach because of the flexibility and the ease of exchanging a new detection module using SrtA-mediated ligation.

In addition to antibody, DNA aptamers have gained considerable attention as a sensitive sensing component since they can be selected to bind many target antigens with specificity and affinity rivaling that of antibodies.[43,44] In addition, DNA can also function as a detection module through hybridization to DNA-modified reporter molecules such as DNA nanobarcodes.[45] To provide a universal platform to incorporate DNA into the E2 nanoprobe, HaloTag was again exploited to conjugate to CH-modified DNA. A MUC1-sepcific DNA aptamer[41] was conjugated to HaloTag, and the DNA-HaloTag-ELP-E2 conjugates were confirmed by detecting a slower mobility band compared with free HaloTag-ELP-E2 protein (Figure 5A). Alexa 488 was further conjugated onto the nanoprobes for detection

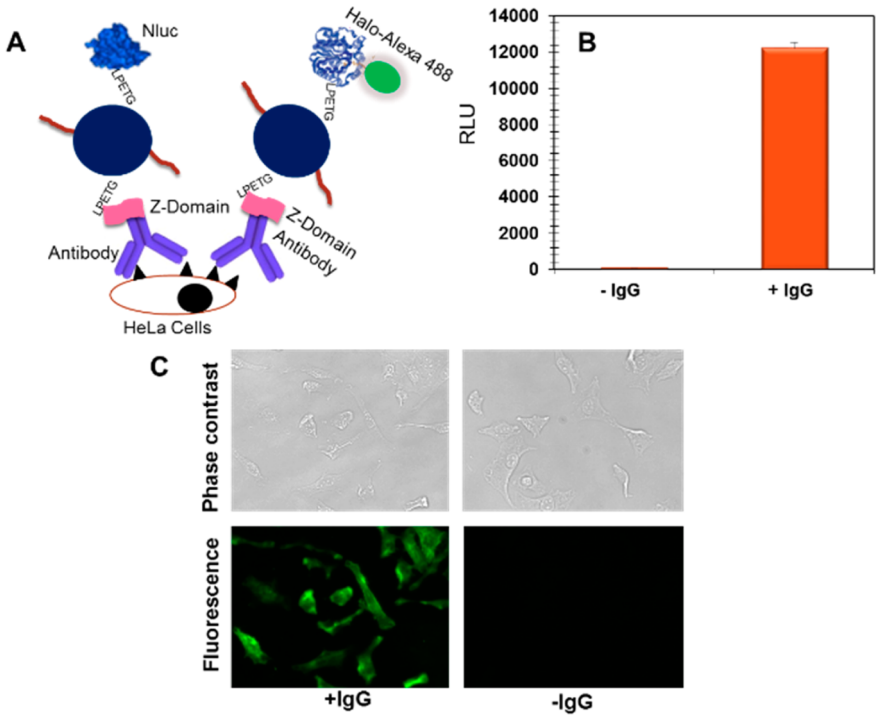

Figure 4. (A) Detection of MUC1 on HeLa cells using E2 nanoprobes. (B) Detection of MUC1 with Nluc as the detection output. (C) Phase contrast and fluorescence images of HeLa cells detection with Alexa 488 as the detection output.

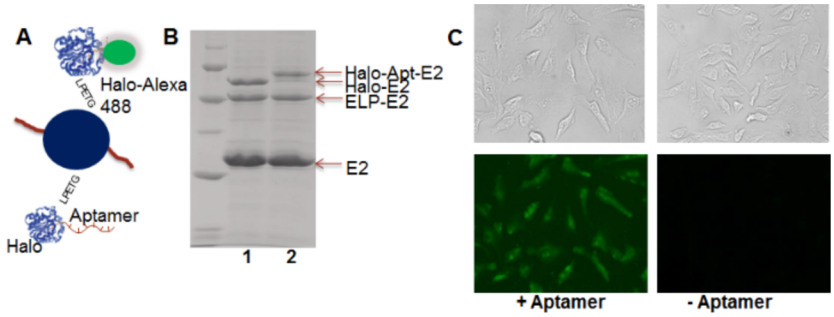

Figure 5. Detection of MUC1 on HeLa cells using DNA aptamers. (A) Conjugation of MUC1 aptamers onto HaloTag-ELP-E2 nanoparticles. (B) Phase contrast and fluorescence images of HeLa cells detection with using MUCI aptamer-modified E2 nanoprobes.

purpose (Figure S7B). Similar to the results with antibody, HeLa cells were detected only with nanoprobes loaded with DNA aptamers (Figure 5B). Since DNA aptamers and Alexa 488 shared the same HaloTag, the fluorescence signal was less compared with that for the antibody and Alexa 488 combination. This can be easily addressed by ligating more HaloTag onto the nanoprobe for improved sensitivity in a fashion similar to the case with Nluc. This is precisely the modularity of our approach in tuning the required ratio and function of individual sensing and detection modules for each unique application.

CONCLUSIONS

In summary, we have presented a modular approach to develop highly sensitive nanoprobes by decorating E2 protein nanoparticles with a wide range of sensing and detection functionalities using SrtA-mediated ligation. The use of Z domain allows not only directional immobilization of antibody by targeting the Fc region, but also the virtually unlimited number of commercially available antibodies for sensing specificity. Similarly, an unlimited number of target-specific DNA aptamers can be conjugated to the nanoprobes using HaloTag. However, the flexibility is beyond just the sensing module. Our approach also provides the feasibility to select either enzymes or fluorescent dyes for detection. The sensitivity can be easily fine-tuned by controlling the number of enzymes or dyes conjugated onto the nanoprobes and the use of more than one detection module is possible because of the modular nature of the approach. The multistep nanoprobe assembly process is further simplified by the ELP-based purification scheme. In addition to the sensing and detection modalities reported, there are many other examples such as single chain variable

fragments, fibronectin type III domains, and fluorescence proteins that can be ligated onto the E2 nanoprobe. Even inorganic gold nanoparticles and quantum dots can be easily coupled by employing specific metal binding peptides to further expand the range of applications that can be addressed using this modular platform.

METHODS

Genetic Manipulation and Expression of All the Proteins and Protein Nanoparticles. *Escherichia coli* strain NEB 5-alpha (NEB #C2987I) was used as the host for genetic manipulations. BL21 (DE3) (Novagen) and BLR (DE3) (Novagen) were used for protein expressions. Details of DNA manipulation and expression procedures can be found in the Supporting Information for GGG-E2, His6-Sortase A, ELP-LPETG, Nluc-LPETG, Z-Ct-LPETG, HaloTag-LPETG.

Ligation of Different Sensor Components onto ELP-E2. To prepare ELP-E2, 1 μM of partially purified E2, 12 μM of ELP-LPETG, and 12 μM of Sortase A were used in a final reaction volume of 400 μL (50 mM Tris, 150 mM NaCl, 60 mM $CaCl_2$, pH 8). Reaction mixtures were incubated at 37 °C for 4 h. The ligated products were collected by inverse phase transition with the addition of 1 M Na_2SO_4, incubated at 37 °C for 10 min, and centrifuged at 160 000*g* for 10 min at 37 °C. After discarding the supernatant, the protein pellets were resolubilized in 4 °C cold buffer. This thermal cycle was repeated for better purity.

To ligate Z-Ct-LPETG onto ELP-E2 (10% E2 monomers ligated with ELP), 1 μM of ELP-E2, 12 μM of Z-Ct-LPETG, and 12 μM of Sortase A were used in a 400 μL reaction volume. The precipitation and resolubilization procedures were the same as ELP-E2 as described above. The resulting products were analyzed with 10% SDS-PAGE. Nluc-LPETG and HaloTag-LPETG ligation onto ELP-E2 were achieved using similar procedures.

Functionality of the Ligated Z-Domain. The functionality of the Z-domain was confirmed by the ability to capture rabbit IgGs.[46] Briefly, 1 μM Z-ELP-E2 was incubated with 20 μM RIgG for 3 h at room temperature before the addition of 1 M NaCl. The mixture was incubated at 28 °C for 10 min and centrifuged for 10 min at 15 000 rpm and 28 °C. The pellet was resuspended in ice-cold binding buffer for resolubilization. Full complex assemblies were visualized by SDS-PAGE analysis and transmission electron microscopy. Samples were prepared in DDI water and stained with 2% uranyl acetate on carbon-coated copper grids (Electron Microscopy Science). Zeiss Libra 120 Transmission Electron Microscope was used to visualize the samples with voltage of 120 kV.

Functionality of the Ligated Nluc. The Nluc activity was confirmed by using the Nano-Glo Luciferase assay system (Promega, Madison, WI), which detects the transfer of Furimazine to Furimamide by Nluc with light emitting as the product. The assay mixture and the Nluc cell lysate were mixed and allowed to equilibrate to room temperature. An equal volume of the Nano-Glo luciferase assay reagent was mixed with the diluted Nluc cell lysate. Luminescence was captured by the Synergy H4 hybrid multimode microplate reader from BioTek (Winooski, VT).

Sensor Assembly. Biosensor assembly was achieved by a sequential ligation procedure. In step 1, ELP-LPETG was ligated onto GGG-E2 to form ELP-E2. In step 2, either Z-Ct-LPETG or HaloTag-LPETG was ligated onto ELP-E2 and purified as described. The decoration efficiency can be adjusted by setting up the ligation mixture with 1 μM ELP-E2 particles, 12 μM of Sortase A and the first protein with concentrations ranging from 12 to 60 μM. By changing the concentration of the first protein in the reaction mixture, the decoration efficiency can be easily adjusted. In step 3, a second protein, either Nluc-LPETG or HaloTag-LPETG, was subsequently ligated to generate the final E2 nanoprobes. Again, the decoration efficiency of the second protein can also be adjusted by changing the protein concentration in the reaction mixture. Overall, this stepwise ligation method for nanoprobe assembly was used to control the correct decoration efficiency of each protein on the particles. The hydrodynamic diameters of the complexes were measured by dynamic light scattering using Zetasizer Nano ZS (Malvern Instruments).

To construct the Z-ELP-E2-HaloTag Alexa 488 nanoprobes for cancer cells detection, sequential ligation was used to generate Z-ELP-E2-HaloTag conjugates. Purified Z-ELP-E2-HaloTag (1 μM) was mixed with 20 μM of CH-modified Alexa 488 at 4 °C overnight for Alexa 488 conjugation. Excess CH-modified Alexa 488 was removed by going through one more thermal cycle purification.

To construct the HaloTag-ELP-E2-Aptamer-Alexa 488 nanoprobes, HaloTag-LPETG was first ligated onto ELP-E2. An anti-MUC1 aptamer, CTT CTC TCT TCC TCT CTC CTT GCA GTT GAT CCT TTG GAT ACC CTG G, modified with a 5′ amine was purchased from Integrated DNA Technologies, Coralville, IA. With the use of the 59 amine group, the aptamer was modified with a Chlorohexane (CH) ligand from Promega (Madison, WI). Briefly, the CH ligand was mixed with the aptamer at a molar ratio of 30:1 and incubated at room temperature for 4 h and 4 °C overnight. Excess CH ligand was removed using a 3000 Da ultrafiltration column (Vivaspin 500, Sartorius Stedim Biotech). CH-modified anti-MUC1 aptamers (10 μM) were mixed with the HaloTag-ELP-E2 conjugates at 4 °C overnight to form HaloTag-ELP-E2-Aptamer. After removing the excess aptamer by thermal purification, CH-Alexa 488 (20 μM) was added and incubated at 4 °C for overnight to form the HaloTag-ELP-E2-Aptamer-Alexa 488 nanoprobes. The labeling efficiency was visualized by SDS-PAGE analysis.

Thrombin Detection. Varying concentration of thrombin was coated onto 96 well plates by incubation at room temperature for 2 h. To minimize nonspecific adsorption, 200 μL of 5% milk was used to block the wells by incubating at 4 °C overnight. For sensing, 100 μL of 15 nM thrombin antibody was added to the wells and incubated for 1 h. E2 nanoprobes decorated with the Z domain and Nluc were added to the wells. After 2 h, unbound E2 nanoprobes were removed and 100 μL of the Nano-Glo luciferase assay reagent was added. Luminescence was measured using a microplate reader. Wells were washed 4 times with TPBS between every step to remove the extra reagent.

Cancer Cell Detection. HeLa cells were obtained from American Type Culture Collection (ATCC). Cells were cultured at 37 °C in 5% CO_2 using 1× autoclavable minimum essential medium (Life Technologies: 11700-077) containing 1 vol % of 7.5% $NaHCO_3$, 2 vol % of 1 M Hepes, 1 vol % of nonessential amino acids (Fisher, SH3023801), 2.5 vol % of Pen/Strep (Fisher, SV30010), 2 vol % of L-glutamine (Fisher, SH3003401) and 10 vol % of FBS (Sigma-Aldrich, F6178).

HeLa cells were seeded into 96 well plates and grown at 37 °C overnight until reaching around 90% confluency. The growth media was removed and cells were washed twice with 1× TBS. Cells were fixed with 100 μL of 4% formaldehyde for 10 min and fixed cells were incubated with 100 μL of 100 mM NH_4Cl to minimize background fluorescence. To minimize background adsorption, 5% milk was used to block unspecific binding. For cancer cell detection, 100 μL of 5 μg/mL anti-MUC1 antibody was used to incubate with HeLa cells for 1 h, washed with TBS, and incubated with 100 μL of 10 nM Z-ELP-E2-Nluc nanoprobe to bind onto antibody. After washing three times with TBS, Nluc activity was detected by measuring luminescence using a microplate reader.

For cancer cell detection using the Z-ELP-E2-HaloTag-Alexa 488 nanoprobes, a similar procedure was used except visualization of cancer cells was conducted using a Zeiss AxioObserver Z1 inverted fluorescence microscope. To use the HaloTag-ELP-E2-Aptamer-Alexa 488 nanoprobes for cancer detection, fixed HeLa cells were incubated with the nanoprobes for 2 h and washed three times with TBS. Cancer cells detection was again

performed using a Zeiss AxioObserver Z1 inverted fluorescence microscope.

Conflict of Interest: The authors declare no competing financial interest.

Supporting Information Available: The Supporting Information is available free of charge on the ACS Publications website at DOI: 10.1021/acsnano.5b03688.

Detailed information on cloning process; figures of detailed three-step ligation for sensor assembly; TEM of raw E2 nanoparticles and IgG associated E2 nanoparticles; Z-Ct-LPETG, HaloTag-LPETG and Nluc-LPETG ligation characterization; sensor assembly and characterization (PDF)

Acknowledgment. We would like to acknowledge the funding support from NSF (CBET1263774 and CBET1264719).

REFERENCES AND NOTES

1. Lazcka, O.; Del Campo, F. J.; Muñoz, F. X. Pathogen Detection: A Perspective of Traditional Methods and Biosensors. *Biosens. Bioelectron.* **2007**, *22*, 1205–1217.
2. Byrne, B.; Stack, E.; Gilmartin, N.; Kennedy, R. O. Antibody-Based Sensors: Principles, Problems and Potential for Detection of Pathogens and Associated Toxins. *Sensors* **2009**, *9*, 4407–4445.
3. Rucker, V. C.; Havenstrite, K. L.; Herr, A. E. Antibody Microarrays for Native Toxin Detection. *Anal. Biochem.* **2005**, *339*, 262–270.
4. Boscolo, S.; Pelin, M.; De Bortoli, M.; Fontanive, G.; Barreras, A.; Berti, F.; Sosa, s.; Chaloin, O.; Bianco, A.; Bianco, T.; et al. Sandwich ELISA Assay for the Quantitation of Palytoxin and Its Analogs in Natural Samples. *Environ. Sci. Technol.* **2013**, *47*, 2034–2042.
5. Cella, L. N.; Sanchez, P.; Zhong, W.; Myung, N. V.; Chen, W.; Mulchandani, A. Nano Aptasensor for Protective Antigen Toxin of Anthrax. *Anal. Chem.* **2010**, *82*, 2042–2047.
6. Hwang, M. P.; Lee, J.-W.; Lee, K. E.; Lee, K. H. Think Modular: A Simple Apoferritin-Based Platform for the Multifaceted Detection of Pancreatic Cancer. *ACS Nano* **2013**, *7*, 8167–8174.
7. Xiang, Y.; Lu, Y. Using Personal Glucose Meters and Functional DNA Sensors to Quantify a Variety of Analytical Targets. *Nat. Chem.* **2011**, *3*, 697–703.
8. Menon, S.; Manning, B. Nutrient Sensing Lost in Cancer. *Nature* **2013**, *498*, 444–445.
9. Xu, J.-J.; Zhao, W.-W.; Song, S.; Fan, C.; Chen, H.-Y. Functional Nanoprobes for Ultrasensitive Detection of Biomolecules: An Update. *Chem. Soc. Rev.* **2014**, *43*, 1601–1611.
10. Tran, T. N. N.; Cui, J.; Hartman, M. R.; Peng, S.; Funabashi, H.; Duan, F.; Yang, D.; March, J. C.; Lis, J. T.; Cui, H.; et al. Universal DNA-Based Protein Detection System. *J. Am. Chem. Soc.* **2013**, *135*, 14008–14011.
11. Tong, S.; Ren, B.; Zheng, Z.; Shen, H.; Bao, G.; Engineering, B.; States, U. Tiny Grains Give Huge Gains: Nanocrystal-Based Signal Amplification for Biomolecule Detection. *ACS Nano* **2013**, *7*, 5142–5150.
12. Su, J.; Xu, J.; Chen, Y.; Xiang, Y.; Yuan, R.; Chai, Y. Personal Glucose Sensor for Point-of-Care Early Cancer Diagnosis. *Chem. Commun. (Cambridge, U. K.)* **2012**, *48*, 6909–6911.
13. Kamiya, N.; Doi, S.; Tanaka, Y.; Ichinose, H.; Goto, M. Functional Immobilization of Recombinant Alkaline Phosphatases Bearing a Glutamyl Donor Substrate Peptide of Microbial Transglutaminase. *J. Biosci. Bioeng.* **2007**, *104*, 195–199.
14. Hess, G. T.; Cragnolini, J. J.; Popp, M. W.; Allen, M. A.; Dougan, S. K.; Spooner, E.; Ploegh, H. L.; Belcher, A. M.; Guimaraes, C. P. M13 Bacteriophage Display Framework That Allows Sortase- Mediated Modi Fi Cation of Surface-Accessible Phage Proteins. *Bioconjugate Chem.* **2012**, *23*, 1478–1487.
15. Parolo, C.; de la Escosura-Muñiz, A.; Polo, E.; Grazu, V.; de la Fuente, J. M. Design, Preparation, and Evaluation of a Fixed-Orientation Antibody/Gold-Nanoparticle Conjugate as an Immunosensing Label. *ACS Appl. Mater. Interfaces* **2013**, *5*, 10753–10759.
16. Sun, Q.; Madan, B.; Tsai, S.-L.; DeLisa, M. P.; Chen, W. Creation of Artificial Cellulosomes on DNA Scaffolds by Zinc Finger Protein-Guided Assembly for Efficient Cellulose Hydrolysis. *Chem. Commun. (Cambridge, U. K.)* **2014**, *50*, 1423–1425.
17. Blackstock, D.; Sun, Q.; Chen, W. Fluorescent Protein-Based Molecular Beacons by Zinc Finger Protein-Guided Assembly. *Biotechnol. Bioeng.* **2015**, *112*, 236–241.
18. Patel, K. G.; Swartz, J. R. Surface Functionalization of Virus-like Particles by Direct Conjugation Using Azide-Alkyne Click Chemistry. *Bioconjugate Chem.* **2011**, *22*, 376–387.
19. Domingo, G. J.; Orru, S.; Perham, R. N. Multiple Display of Peptides and Proteins on a Macromolecular Scaffold Derived from a Multienzyme Complex. *J. Mol. Biol.* **2001**, *305*, 259–267.
20. Ton-That, H.; Mazmanian, S. K.; Alksne, L.; Schneewind, O. Anchoring of Surface Proteins to the Cell Wall of Staphylococcus Aureus. Cysteine 184 and Histidine 120 of Sortase Form a Thiolate-Imidazolium Ion Pair for Catalysis. *J. Biol. Chem.* **2002**, *277*, 7447–7452.
21. Swee, L. K.; Guimaraes, C. P.; Sehrawat, S.; Spooner, E.; Barrasa, M. I.; Ploegh, H. L. Sortase-Mediated Modification of DEC205 Affords Optimization of Antigen Presentation and Immunization against a Set of Viral Epitopes. *Proc. Natl. Acad. Sci. U. S. A.* **2012**, *110*, 1428–1433.
22. Proft, T. Sortase-Mediated Protein Ligation: An Emerging Biotechnology Tool for Protein Modification and Immobilisation. *Biotechnol. Lett.* **2010**, *32*, 1–10.
23. Chen, Q.; Sun, Q.; Molino, N. M.; Wang, S.-W.; Boder, E.; Chen, W. Sortase A-Mediated Multi-Functionalization of Protein Nanoparticles. *Chem. Commun.* **2015**, *51*, 12107–12110.
24. Milne, J. L. S.; Shi, D.; Rosenthal, P. B.; Sunshine, J. S.; Domingo, G. J.; Wu, X.; Brooks, B. R.; Perham, R. N.; Henderson, R.; Subramaniam, S. Molecular Architecture and Mechanism of an Icosahedral Pyruvate Dehydrogenase Complex: A Multifunctional Catalytic Machine. *EMBO J.* **2002**, *21*, 5587–5598.
25. Izard, T.; Aevarsson, A.; Allen, M. D.; Westphal, A. H.; Perham, R. N.; de Kok, A.; Hol, W. G. Principles of Quasi-Equivalence and Euclidean Geometry Govern the Assembly of Cubic and Dodecahedral Cores of Pyruvate Dehydrogenase Complexes. *Proc. Natl. Acad. Sci. U. S. A.* **1999**, *96*, 1240–1245.
26. Liu, F.; Tsai, S.-L.; Madan, B.; Chen, W. Engineering a High-Affinity Scaffold for Non-Chromatographic Protein Purification *via* Intein-Mediated Cleavage. *Biotechnol. Bioeng.* **2012**, *109*, 2829–2835.
27. Lim, D. W.; Trabbic-carlson, K.; Mackay, J. A.; Chilkoti, A. Improved Non-Chromatographic Purification of a Recombinant Protein by Cationic Elastin-like Polypeptides. *Biomacromolecules* **2007**, *8*, 1417–1424.
28. Wenger, M. D.; Dephillips, P.; Price, C. E.; Bracewell, D. G. An Automated Microscale Chromatographic Purification of Virus-like Particles as a Strategy for Process Development. *Biotechnol. Appl. Biochem.* **2007**, *47*, 131–139.
29. Vicente, T.; Roldão, A.; Peixoto, C.; Carrondo, M. J. T.; Alves, P. M. Large-Scale Production and Purification of VLP-Based Vaccines. *J. Invertebr. Pathol.* **2011**, *107*, S42–S48.
30. Braisted, A. C.; Wells, J. A. Minimizing Binding Protein. *Proc. Natl. Acad. Sci. U. S. A.* **1996**, *93*, 5688–5692.
31. Los, G. V.; Encell, L. P.; Mcdougall, M. G.; Hartzell, D. D.; Karassina, N.; Zimprich, C.; Wood, M. G.; Learish, R.; Ohana, R. F.; Urh, M.; et al. Halo Tag: A Novel Protein Labeling Technology for Cell Imaging and Protein Analysis. *ACS Chem. Biol.* **2008**, *3*, 373–382.
32. Blackstock, D.; Chen, W. Halo-Tag Mediated Self-Labeling of Fluorescent Proteins to Molecular Beacons for Nucleic Acid Detection. *Chem. Commun.* **2014**, *50*, 13735–13738.
33. Hall, M. P.; Unch, J.; Binkowski, B. F.; Valley, M. P.; Butler, B. L.; Wood, M. G.; Otto, P.; Zimmerman, K.; Vidugiris, G.; Machleidt, T.; et al. Engineered Luciferase Reporter from a Deep Sea Shrimp Utilizing a Novel Imidazopyrazinone Substrate. *ACS Chem. Biol.* **2012**, *7*, 1848–1857.

34. Tsai, S.; Oh, J.; Singh, S.; Chen, R.; Chen, W. Functional Assembly of Minicellulosomes on the Saccharomyces Cerevisiae Cell Surface for Cellulose Hydrolysis and Ethanol Production. *Appl. Environ. Microbiol.* **2009**, *75*, 6087–6093.
35. Wang, X.; Zhao, Q. A Fluorescent Sandwich Assay for Thrombin Using Aptamer Modified Magnetic Beads and Quantum Dots. *Microchim. Acta* **2012**, *178*, 349–355.
36. Choi, D.; Jeong, H.; Kim, K. Electrochemical Thrombin Detection Based on the Direct Interaction of Target Proteins and Graphene Oxide as an Indicator. *Analyst* **2014**, *139*, 1331–1333.
37. Shimada, J.; Maruyama, T.; Kitaoka, M.; Kamiya, N.; Goto, M. Microplate Assay for Aptamer-Based Thrombin Detection Using a DNA-Enzyme Conjugate Based on Histidine-Tag Chemistry. *Anal. Biochem.* **2012**, *421*, 541–546.
38. Abe, K.; Murakami, Y.; Tatsumi, A.; Sumida, K.; Kezuka, A.; Fukaya, T.; Kumagai, T.; Osawa, Y.; Sode, K.; Ikebukuro, K. Enzyme Linking to DNA Aptamers *via* a Zinc Finger as a Bridge. *Chem. Commun.* **2015**, *51*, 11467–11469.
39. Yin, J.; Zhang, A.; Dong, C.; Ren, J. An Aptamer-Based Single Particle Method for Sensitive Detection of Thrombin Using Fluorescent Quantum Dots as Labeling Probes. *Talanta* **2015**, *144*, 13–19.
40. Mcauley, J. L.; Linden, S. K.; Png, C. W.; King, R. M.; Pennington, H. L.; Gendler, S. J.; Florin, T. H.; Hill, G. R.; Korolik, V.; Mcguckin, M. A. MUC1 Cell Surface Mucin Is a Critical Element of the Mucosal Barrier to Infection. *J. Clin. Invest.* **2007**, *117*, 2313–2324.
41. Ferreira, C. S. M.; Matthews, C. S.; Missailidis, S. DNA Aptamers That Bind to MUC1 Tumour Marker: Design and Characterization of MUC1-Binding Single-Stranded DNA Aptamers. *Tumor Biol.* **2006**, *27*, 289–301.
42. Painter, J. T.; Clayton, N. P.; Herbert, R. a. Useful Immunohistochemical Markers of Tumor Differentiation. *Toxicol. Pathol.* **2010**, *38*, 131–141.
43. Deng, B.; Lin, Y.; Wang, C.; Li, F.; Wang, Z.; Zhang, H.; Li, X. F.; Le, X. C. Aptamer Binding Assays for Proteins: The Thrombin Example-A Review. *Anal. Chim. Acta* **2014**, *837*, 1–15.
44. Germer, K.; Leonard, M.; Zhang, X. RNA Aptamers and Their Therapeutic and Diagnostic Applications. *Int. J. Biochem. Mol. Biol.* **2013**, *4*, 27–40.
45. Li, Y.; Cu, Y. T. H.; Luo, D. Multiplexed Detection of Pathogen DNA with DNA-Based Fluorescence Nanobarcodes. *Nat. Biotechnol.* **2005**, *23*, 885–889.
46. Madan, B.; Chaudhary, G.; Cramer, S. M.; Chen, W. ELP-Z and ELP-Zz Capturing Scaffolds for the Purification of Immunoglobulins by Affinity Precipitation. *J. Biotechnol.* **2013**, *163*, 10–16.